Int J Coal Sci Technol (2021) 8(6):1447–1460
https://doi.org/10.1007/s40789-021-00456-y

An exsitu underground coal gasification experiment with a siderite interlayer: course of the process, production gas, temperatures and energy efficiency

Marian Wiatowski[1] · Krzysztof Kapusta[1] · Jacek Nowak[2] · Marcin Szyja[1] · Wioleta Basa[1]

Received: 11 December 2020 / Revised: 11 June 2021 / Accepted: 2 July 2021 / Published online: 10 August 2021

Abstract A 72-h ex situ hard coal gasification test in one large block of coal was carried out. The gasifying agent was oxygen with a constant flow rate of 4.5 m^3/h. The surroundings of coal were simulated with wet sand with 11% moisture content. A 2-cm interlayer of siderite was placed in the horizontal cut of the coal block. As a result of this process, gas with an average flow rate of 12.46 m^3/h was produced. No direct influence of siderite on the gasification process was observed; however, measurements of CO_2 content in the siderite interlayer before and after the process allow to determine the location of high-temperature zones in the reactor. The greatest influence on the efficiency of the gasification process was exerted by water contained in wet sand. At the high temperature that prevailed in the reactor, this water evaporated and reacted with the incandescent coal, producing hydrogen and carbon monoxide. This reaction contributes to the relatively high calorific value of the resulting process gas, averaging 9.41 MJ/kmol, and to the high energy efficiency of the whole gasification process, which amounts to approximately 70%.

Keywords Underground coal gasification · UCG · Siderite interlayer · Water · Ex situ · Hydrogen

1 Introduction

Underground coal gasification (Bhutto et al. 2013; Cena and Thorness 1981; Perkins 2018) consists of the reaction of the oxidizing reagent (mainly oxygen) and water with the raw coal located underground, which results in the production of process gas and byproducts such as post-process water and tar substances. The main idea of the process is to obtain as much process gas as possible with highest calorific value. Depending on the gasification conditions, the obtained process gas contained 10%–30% H_2, 15%–25% CO, 5%–8% CH_4 and 15%–60% CO_2 (Su et al. 2017; Wang et al. 2008). After cleaning, this gas can be a valuable raw material for the chemical industry (Gregg and Edgar 1978; Maev et al. 2018). The course of this process is influenced by many factors, the most important of which are the oxygen concentration in the gasifying agent and its flow rate, process pressure and temperature, coal composition and geological conditions (Blinderman and Friedmann 2006; Kreinin et al. 1982). From the literature (Hamanaka et al. 2017; Huang et al. 2021; Shu et al. 2020), it is known that the higher the concentration of oxygen in the gasifying agent, the higher the temperature, and in turn the higher the concentration of CO and H_2 process gas. When it comes to CO_2 concentration, at a low reaction pressure, with a temperature increase from about 650 °C, the carbon dioxide reacts according to the Boudouard reaction, as a result of which the CO_2 content decreases and CO increases. However, if there is too much oxygen, the CO_2 concentration will also increase. At high pressures, the Boudouard reaction takes place to a much lesser extent, and then the increased pressure has little effect on lowering the CO_2 concentration. As for the

✉ Marian Wiatowski
mwiatowski@gig.eu

[1] Główny Instytut Górnictwa (Central Mining Institute), Plac Gwarków 1, 40-166 Katowice, Poland

[2] Politechnika Śląska, Katedra Geologii Stosowanej (Institute of Applied Geology, Silesian Technical University), ul. Akademicka 2A, Gliwice, Poland

concentration of CH_4, steam is needed in methanation processes and appropriate process conditions must be maintained, with pressure and temperature playing a crucial role. With pressure increases, the concentration of methane increases and the concentration of hydrogen decreases, because hydrogen is consumed in the methanation reaction. As the methanation processes are exothermic, too high a temperature will not favor the formation of methane (Kapusta et al. 2020; Roberts and Harris 2000; Wall et al. 2002; Wiatowski et al. 2016).

Regarding the gasification temperature, the literature data (Kapusta et al. 2016; Su et al. 2017; Wang et al. 2008) show that the temperature during gasification of coal with air may reach up to 1200 °C, and in the case of gasification with oxygen-enriched air, it may be even higher.

The temperature distribution in the UCG reactor depends on the reaction zone, which is divided into an oxidation, reduction and a dry. Depending on the gasification conditions, the literature gives different temperature values in individual gasification zones. In the work (Bhutto et al. 2013), the temperature range in the oxidation zone was 900–1450 °C, in the reduction zone: 600–100 °C and in the drying zone: 200–600 °C. In another study (Wang et al. 2017), during gasification of lignite with oxygen and CO_2, the temperatures in the oxidation zone exceeded 900 °C, in the reduction zone they were 600–900 °C, and in the drying zone: 300–600 °C. The results of various experiments of coal gasification with different yield and calorific value of the process gas obtained are reported in the literature. For example, in the test of underground hard coal gasification on a mine "Barbara" (Wiatowski et al. 2015) using oxygen, the average calorific value of the gas was 8.08 MJ/m^3 with a gasification capacity of 2.06 m^3/kg of coal. In another hard coal gasification experiment, on a mine "Wieczorek" (Mocek et al. 2016), using oxygen, oxygen-enriched air and CO_2, the average calorific value of the gas was 3.38 MJ/m^3 with the gasification efficiency of 4.6 m^3/kg of coal. In the former Soviet Union, at the Podzemgaz South Abińsk station (Olness 1982), during gasification of coal with air, the calorific value of the gas obtained was in the range of 2.9–3.4 MJ/m^3 and gas production was 2.67 m^3/kg of coal gasified.

As far as the role of water (Dvornikova 2018; Perkins and Prabu 2017; Surya and Prabu 2017) in underground gasification is concerned, it is essential because it is the raw material from which H_2 and CO are produced. Reactions in which water is essential are described by the following equations:

$$C + H_2O \rightarrow CO + H_2 \quad \Delta H = +135.7 \text{ kJ/kmol} \tag{1}$$

$$CO + H_2O \rightarrow CO_2 + H_2 \quad \Delta H = -33.2 \text{ kJ/kmol} \tag{2}$$

Equation (1) is endothermic, while Eq. (2) is slightly exothermic. The source of water is the moisture contained in coal and water inflowing to the gasified seam. If there is a lack of water, it has to be supplied from the outside; but on the other hand, when there is too much water, the temperature in the gasified seam decreases and the consumption of heat energy necessary to evaporate the excess water increases (Daggupati et al. 2011). Evaporated water in the form of steam increases the moisture content of the process gas, making it necessary to remove excess water in the gas purification process. In addition, the presence of a large amount of steam in the gas increases its volume, which increases the cost of gas transport. At low process gas temperatures, steam may condense inside the pipeline, transporting the gas. This can, in extreme cases, result in water and tar jams, which are not beneficial for this process. All phenomena related to excess water cause an increase in energy consumption, which in the final effect reduces the efficiency of the process.

Another factor influencing the UCG process is the composition and properties of the gasified coal. Hard coal (Chodyniecka and Walanus 1985; Elliott 1981) is a very complicated mixture of organic carbon substances, mineral substances and moisture. The mineral substances contained in coal may affect the course of gasification (Bhutto et al. 2013; Karimi and Gray 2011; Mandapati et al. 2012). One of the minerals usually found in coal is siderite (Retallack 2007). Its main component is iron (up to 48%) in the form of iron carbonate $FeCO_3$. Most often, such siderite is partially oxidized, which is manifested by its brown colour. Apart from iron, siderite often contains elements such as Si, Al, Mg and Ca. Siderite in coal may occur in the form of discontinuous inserts, thin layers, sideritized laystones and mudstones or nodules made of compactedoolite-type siderites (Maes et al. 2000). Hard coal may have a siderite content between zero and a few percent. In a study (Riley et al. 2012) concerning research on Australian bituminous coals, the siderite content was 0.11%–2.72%. Siderite is also found in rocks accompanying coal seams in the form of clusters of variable thickness between 2 and 40 cm. Its content in these rocks may be higher than the content in coal and can reach several dozen percent (Chodyniecka and Gabzdyl 1986).

Under high-temperature conditions that occur during UCG, the siderite undergoes thermal decomposition (Dhupe and Gokarn 1990) to wustite. Siderite decomposition is an endothermic reaction that occurs at temperatures of 350–530 °C according to a simplified equation (variant I):

$$FeCO_3 \leftrightarrow FeO + CO_2 \quad \Delta H = +88.12 \text{ kJ/kmol} \tag{3}$$

The resulting iron oxide FeO may react with carbon dioxide to magnetite:

$$3FeO + CO_2 \leftrightarrow Fe_3O_4 + CO \quad \Delta H = -24.31 \text{ kJ/kmol} \tag{4}$$

In variant II (Zhu et al. 2016), siderite may decompose according to the following equation:

$$3FeCO_3 \rightarrow Fe_3O_4 + 2CO_2 + CO \quad \Delta H = +240.05 \text{ kJ/kmol} \tag{5}$$

The resulting magnetite may undergo the opposite reaction described in Eq. (4) to wustite. Siderite can also react with the hydrogen contained in the process gas according to the following equation:

$$FeCO_3 + H_2 \rightarrow Fe + CO_2 + H_2O \quad \Delta H = +116.67 \text{ kJ/kmol} \tag{6}$$

If the decomposition of siderite takes place in an atmosphere containing oxygen, at 600–750 °C, iron is oxidized to magnetite (Lee et al. 2009). This reaction is exothermic and can be described by the following equation:

$$3FeO + 1/2O_2 \leftrightarrow Fe_3O_4 \quad \Delta H = -307.29 \text{ kJ/kmol} \tag{7}$$

The iron oxides formed from siderite have a catalytic effect (Smirnov et al. 2019; Wang et al. 2016; Yang et al. 2009) in the reaction of water gas conversion (Eq. (2)) and the endothermic Bouduard reaction:

$$C + CO_2 \leftrightarrow 2CO \quad \Delta H = +169.9 \text{ kJ/kmol} \tag{8}$$

The catalytic properties are dependent on the degree of surface development and contact with substrates. If iron oxides are small in size and dispersed in coal, they can have a catalytic effect. If they are concentrated in one place in the form of larger grains, then the catalytic effect will be marginal (Smirnov et al. 2019).

The Bouduard reaction (Eq. (8)) is reversible and only occurs at low pressures above 650 °C. From the equations presented, it follows that the decomposition of siderite causes the release of CO_2. If the siderite is located close to the high-temperature zone, the sample taken after the gasification process should contain a lower amount of CO_2 than before the process. It is therefore possible, if only in a very approximate way, to determine the location of high-temperature zones in the reactor. Under real conditions, this is not feasible, but during the exsitu gasification process, such an experiment is possible.

The main purpose of this study was to investigate the effect of siderite addition on the course of the underground coal gasification process in ex situ conditions and to attempt to determine the temperature distribution in the UCG reactor. The impact of moisture contained in the surroundings of the gasified coal seam on the composition and yield of the process gas was also determined. Research on the influence of siderite and the mapping of temperatures in the UCG process described in this work has not been conducted thus far. The results obtained can therefore contribute to the expansion of knowledge in this field of science.

2 Experimental

2.1 Installation for ex situ coal gasification

The coal gasification test was conducted in an experimental reactor designed to simulate the UCG process under surface conditions. The installation enables leading of the underground coal gasification process on the surface (ex situ) in a simulated coal seam (max. seam length 7.0 m, crosssection 1.0 m × 1.0 m) under atmospheric pressure. The maximum design process temperature can be up to 1600 °C. The gasification reactor was equipped with appropriate technical infrastructure to carry out the gasification process (gasification agent dosing system, takeoff, cleaning and disposal of the resulting process gas). Gasification tests can be carried out using oxygen, air and steam, either individually or in mixtures. Nitrogen is used to inertise the installation and in the final phase to cool the reactor after the process. In order to quickly remove the volatile gasification products from the reaction zone, the process installation was equipped with a suction fan. By reducing the residence time of the volatile products in the reactor, the possible risk of partial combustion flammable components of the process gas in the oxygen stream was down. A schematic view of the installation is presented in Fig. 1, and details of the reactor construction are shown in Fig. 2.

The process gas was treated in a dedicated separation and purification module, the first element of which was a water scrubber (quick gas cooling and condensation of process tars). Next, the gas was directed to an air cooler, moisture separators, oily substances and solid particles.

Part of the gas stream was directed through a separate gas path for chemical analysis, where concentrations of basic gas components such as hydrogen, carbon monoxide and dioxide, methane, ethane and hydrogen sulfidewere determined by chromatographic methods. The temperature profiles inside the reactor were measured using a set of up to 18 thermocouples placed at different heights of the simulated coal seam and overburden layer. The length of each thermocouple (0.45 m) was selected so that it is possible to measure the temperature as close as possible to the fire channel both inside and outside the gasified bed. The arrangement of thermocouples in the reactor are shown in Fig. 2a,c. The white circles in Fig. 2a indicate the places

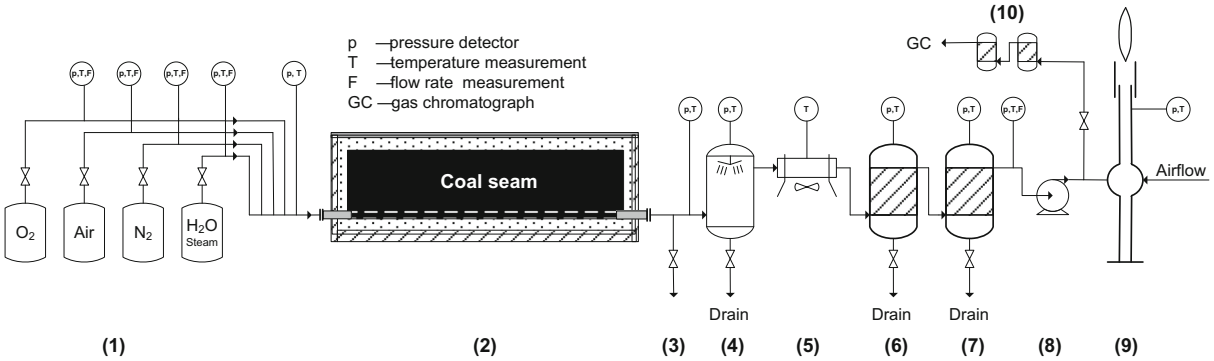

Fig. 1 Scheme of ex situ UCG installation: (1) reagent supply system, (2) gasification reactor, (3) connection for tar sampling, (4) water scrubber, (5) air cooler for process gas, (6,7) gas separators, (8) centrifugal suction fan, (9) thermal combustor, (10) gas purification module for GC analysis

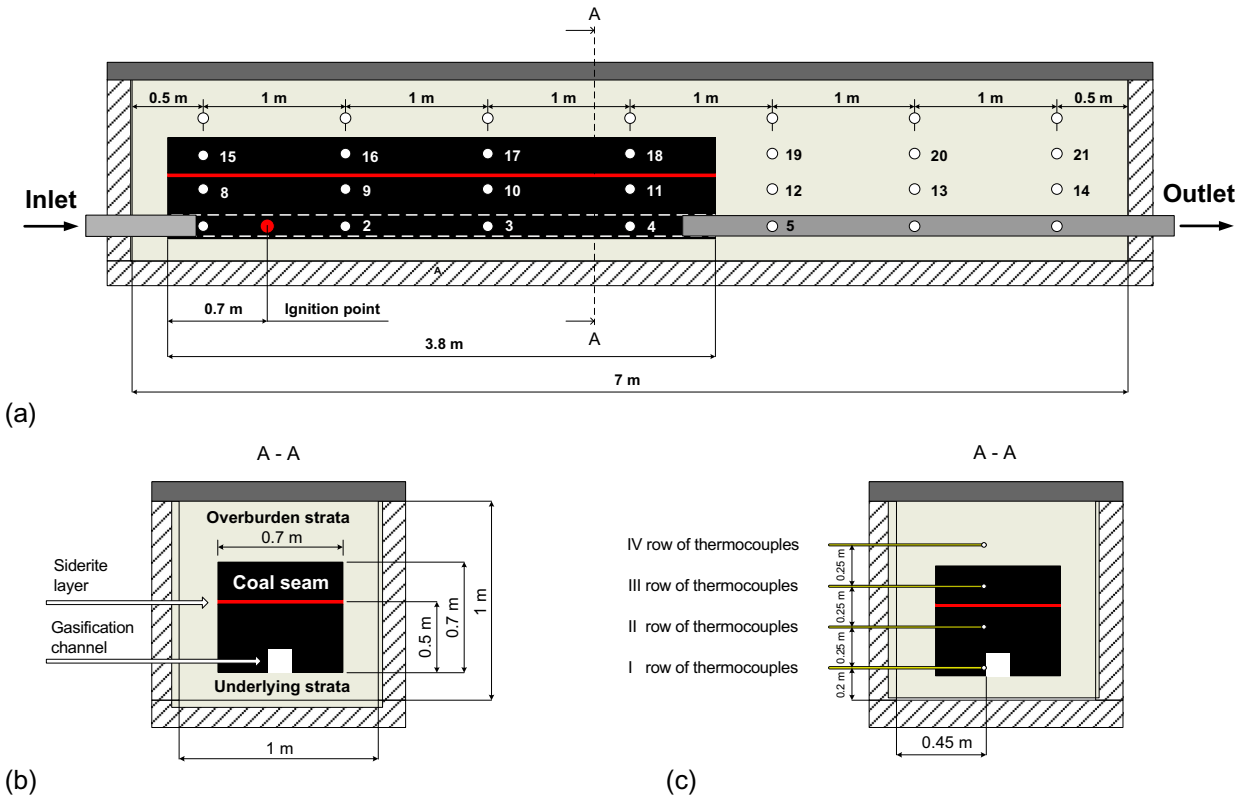

Fig. 2 Details of reactor construction: **a** longitudinal cross section: arrangement of coal seam and thermocouple positions, **b**,**c** cross-section: dimensions of coal seam and thermocouple distances

constructive designed for thermocouples, while the numbers next to the circles indicate the thermocouples actually used in this process. The first row of thermocouples (T2–T5) was located at the level of the fire duct at a distance of 0.2 m from the bottom of the reactor. The second and third rows of thermocouples (T8–T14 and T15–T21) were placed every 0.25 m higher. The T1 thermocouple, which was closest to the oxygen inlet, had to be removed from the reactor due to its unfavorable arrangement with respect to the supply pipe.

The control equipment recorded data every 10 s. All results obtained for gas products were converted to normal conditions (T = 273.15 K, p = 1013.25 hPa).

2.2 Materials

As a material for the gasification test, hard coal "Piast" was used, and the mineral interlayer was a layer of siderite. The insulation of the gasified coal from the reactor walls was wet sand, which filled the empty spaces of the reactor

and simulated the moisture of the surroundings of the gasified coal. The gasifying agent was technical oxygen of 99.95% purity taken from the bundle of oxygen cylinders. The basic properties of the "Piast" hard coal used for gasification are presented in Table 1. Analysis of coal was carried out in a certified laboratory at Silesian Technical University according to Polish Standards.

The raw coal used was characterized by low moisture (as received) at 4.7%, a relatively high content of ash at 16.30% and volatile parts at 30.10%. The lower heating value of coal was 22,719 kJ/kg. Because the raw coal did not contain siderite, it was necessary to deliver it from outside. The siderite used to make the interlayer was a mixture of several siderites from the area of the Chwałowice Basin, from the Rudzkie layers. It was obtained from a heap located on the border of the Marklowice and Świerklany communes using mining waste from deposits 408 and 409 of the Chwałowice mine. Prior to the gasification process, the elemental chemical composition in the siderite interlayer was determined using X-ray fluorescence (XRF) from the ZSX Primus II Rigaku spectrometer, and the results were converted into oxides, while the CO_2 content was determined by the volumetric method in the Scheibler–Dietrich apparatus. The method consists of measuring the volume of CO_2 released during the reaction of the tested sample with hydrochloric acid. To obtain accurate results of the CO_2 content in the siderite interlayer, samples for analysis were taken every 0.2 m (measuring grid 0.2 m × 0.2 m). In total, approximately 80 samples were analysed. The obtained results showed that the tested siderites were characterized by similar CO_2 content in the range of 33.1%–35.7% by mass and 34.6% on average. The detailed mineral composition of the siderites is presented in Table 2.

The data show that the dominant component is iron oxide (41.08% FeO). The content of other minerals was much lower and amounted (up to 1% by mass): silicon dioxide (10.72%), aluminium trioxide (5.03%), magnesium oxide (3.33%) and calcium oxide (2.37%).

Table 1 Proximate and ultimate characteristics of coal from Piast mine and standard analytical methods

Parameter	Value	Standard[b]
As received		
Total moisture W_t^r (%)	4.70	PN-G-04511:1980
Ash A_t^r (%)	16.30	PN-G-04560:1998
Volatiles matter V_r^a (%)	30.10	PN-G-04516:1998
Total sulphur S_t^r (%)	0.83	PN-G-04584:2001
Lower heating value Q^r (kJ/kg)	22 719	PN-G-04513:1981
Analytical		
Moisture W^a (%)	2.95	PN-G-04560:1998
Ash A^a (%)	16.60	PN-G-04560:1998
Volatiles matter V^a (%)	30.65	PN-G-04516:1998
Lower heating value Q^a (kJ/kg)	23 137	PN-G-04513:1981
Total sulphur S_t^a (%)	0.85	PN-G-04584:2001
Carbon C^a (%)	62.50	PN-G-04571:1998
Hydrogen H^a (%)	4.39	PN-G-04571:1998
Nitrogen N^a (%)	1.04	PN-G-04571:1998
Oxygen O^a* (%)	11.67	

Note r received, *t* total, *a* analytical, *b* Polish testing by the accredited laboratory

*Oxygen calculated as $(O^a) = 100 - (W^a) - (A^a) - (C^a) - (H^a) - (S_t^a) - (N^a)(\%)$

2.3 Preparation of coal seam with siderite interlayer and reactor for gasification

The block of coal used for gasification was 3.8 m long, 0.7 m wide and 0.7 m high. It was cut horizontally at a height of 0.5 m counting from underneath. The 2-cm-thick siderite interlayer was placed in the cutting of the block. The weights of the blocks of coal and siderite were 2300 kg and 150 kg, respectively. To fill the empty space in the reactor, 7900 kg of wet sand of 11.0% humidity was used. The moisture content in the sand was measured according to the PN-G-04511:1980 standard.

2.4 Apparatus for measuring physicochemical properties of gaseous media

The list of the equipment and measurement methods used is presented in Table 3.

Table 2 Average composition of used mixture of siderites

Component	Composition (wt%)
FeO	41.08
SiO_2	10.72
Al_2O_3	5.03
MgO	3.33
CaO	2.37
Na_2O	0.79
MnO	0.63
K_2O	0.47
P_2O_5	0.43
Cl	0.24
TiO_2	0.19
SO_3	0.05
BaO	0.03
SrO	0.02
ZnO	0.02
CO_2	34.60
Total	100.00

2.5 Experimental procedure

The experiment began with switching on the suction fan and then igniting the coal seam with a pyrotechnic charge. Coal ignition was carried out with the use of a pyrotechnic charge (Hildebrandt 2015) developed for the needs of the Central Mining Institute's previous research programs in the area of underground coal gasification. The incendiary charge was placed 0.7 m from the beginning of the coal block. The ignition process was started with an oxygen flow rate of 2 m^3/h. After igniting the coal, the oxygen flow was increased to 4 m^3/h. The incendiary charge consisted of 800 g granulated pyrotechnic mass used in explosives used in underground mining. Appropriate modification of the composition of this mass allowed to achieve a relatively long burning time of 3–5 min at a temperature of 800–900 °C. The pyrotechnic mass was ignited by two fuses actuated by a capacitor electric igniter through wires led outside the reactor. The process initiation was considered complete when the oxygen concentration in the process gas decreased to a value lower than 1%. Next, the oxygen flow rate was set at 4.5 m^3/h, and this value was kept constant throughout the experiment. To prevent clogging of the process gas pipes by the liquefied tar, a pump feeding water to the scrubber was switched on simultaneously (water injection 14 kg/h). Every 2 h, the scrubber was emptied, and the amount of wastewater received was weighed. The gas produced was analysed every hour or more often as required. After three days of the gasification process (72 h), the oxygen supply was stopped, and nitrogen in the amount of 2 m^3/h was started until the gasified coal seam was cooled down (to internal temperatures below 100 °C). After the gasification test was completed, the reactor was disassembled, the sand overburden was removed, its moisture content was examined, and samples of thermally transformed siderites were taken to analyse the CO_2 content.

3 Results and discussion

3.1 Process gas flow and gas calorific value

Figures 3 and 4 show the flow of the process gas obtained and its calorific value.

The data received (Fig. 3) show that from the beginning of the process until approximately 46 h, the flow of gas received was relatively stable and amounted to 10–14 m^3/h. After 46 h of the process, the amount of gas produced started to increase to the final value of approximately 18 m^3/h. The total amount of gas produced was 896.94 m^3 with an average flow of 12.46 m^3/h. The calorific value of the gas (Fig. 4) showed a downward trend from 5 and 46 h. Between the next 46–64 h of the process, there was an upward trend in the calorific value of the gas; then, after 64 h, the calorific value decreased slightly until the end of the experiment. During the entire gasification period, quite rapid increases and decreases in caloric value were visible. For example, between 25–28 h and 56–58 h of the process, the calorific value of the gas increased from approximately 9–10.5 MJ/m^3 and from 9–11 MJ/m^3, respectively. The calorific value of the gas obtained was very high, ranging from 8–11 MJ/m^3, while the average value over the entire gasification period was 9.41 MJ/m^3.

3.2 Process gas composition and mass flow of its components

Measurements of the composition of the obtained gas are presented in Fig. 5, while the mass stream of its individual components is presented in Fig. 6.

The data presented in Fig. 5 show that the composition of the gas produced was quite stable throughout the gasification process. Between 25–28 h and from approximately 46 h of the process, a significant decrease in carbon dioxide content was observed with a simultaneous increase in hydrogen and carbon monoxide content. From approximately 46 h of gasification, the methane content started to gradually increase, and after 60 h, it stabilized at a value of approximately 5%. Changes in the concentrations of

Table 3 List of used equipment and measurement methods

Measured value	Control method
Gas temperature inside the reactor	Thermocouple Pt10Rh-Pt
Temperature at the reactor inlet, outlet and scrubber	Resistance sensor Pt100
Pressure	WIKA digital transmitter IS-20-S
Flow of process gas	ELSTER bellows gasometer BK-G10M
Composition of process gases	Agilent 3000A gas chromatograph
Flow of oxygen	Bronkhorst EL-FLOW mass flow controller, model F-202AV-M20-RAD

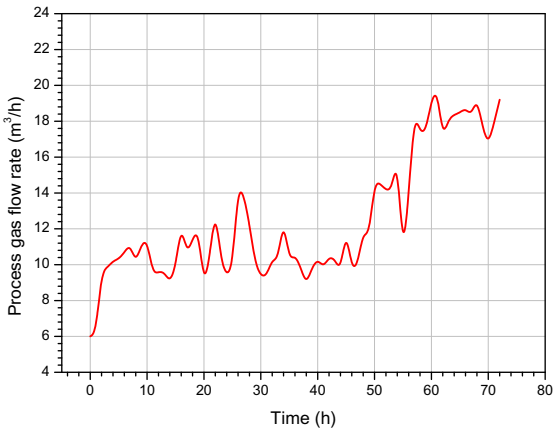

Fig. 3 Process gas flow rate

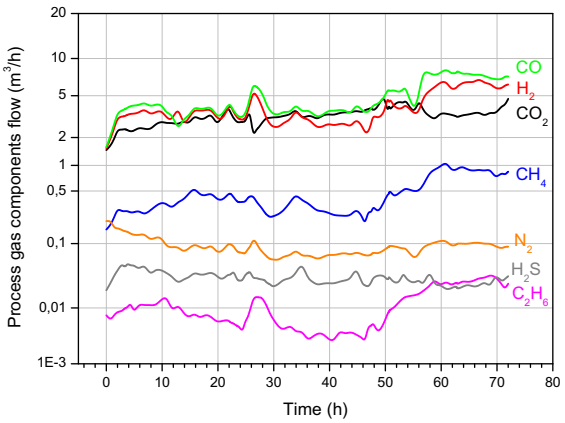

Fig. 6 Mass flow of process gas components

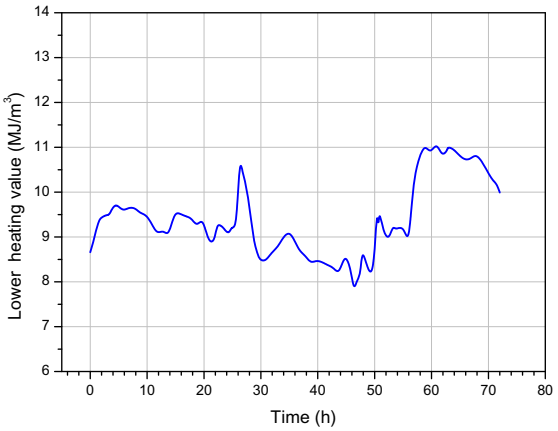

Fig. 4 Process gas calorific value

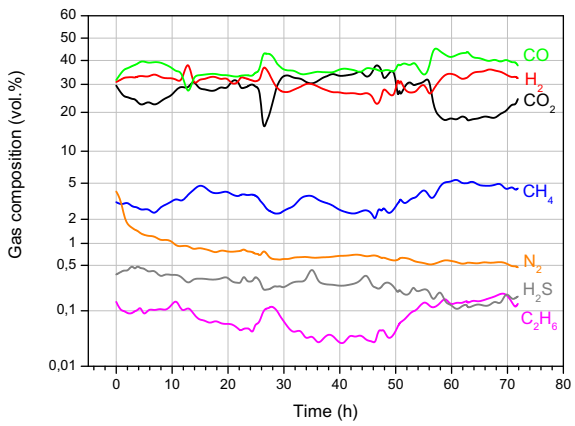

Fig. 5 Composition of process gas

process gas components caused an increase in its calorific value (Fig. 4) in the given time intervals. Throughout the whole experiment, high concentrations of hydrogen (23%–38%) and carbon monoxide (27%–46%) were observed. The methane concentration during the whole process was in the range of 2%–5.6%, while the content of ethane and hydrogen sulfide was practically below 0.5% and 0.2%, respectively.

Figure 6 shows that the hydrogen and carbon monoxide flow increased twice between 25–28 h and twice from 46 h to the end of the gasification process. As far as methane is concerned, in the second half of the gasification process, a clear increase in its flow was observed. From approximately 46 h to the end of gasification, the flow of methane increased by up to three times in the same period of time as the increase in flow of hydrogen and carbon monoxide. The relationships presented in Fig. 6 describe the changes in process gas during the gasification process in more detail than in Fig. 5 because they take into account the concentrations of individual components of the process gas and their flow.

The average composition of the process gas is shown in Table 4. Notably, the high average content of hydrogen and carbon monoxide and low CO_2 content are similar to those in the UCG process.

3.3 Amount of water obtained and humidity of process gas

As a result of coal gasification, in addition to gas, process water was obtained. The amount of this water produced and the gas moisture content calculated on this basis are shown in Fig. 7. The data presented only relate to the amount of water that entered the scrubber from the reactor due to evaporation and subsequent condensation, which was created as a result of chemical reactions occurring during gasification. The amount of water that was injected into the scrubber to cool hot gases was subtracted. At the beginning of gasification, the mass of condensate liquefied grows quickly and then drops rapidly. It reaches a minimum of 4.5 kg/h in 10 h. This stage is related to the evaporation of

Table 4 Composition of process gas and its calorific value

Average composition of process gas (vol%)							Lower heating value Q (MJ/m^3)
CO_2	N_2	H_2	CH_4	CO	C_2H_6	H_2S	
27.27	0.80	30.93	3.53	37.11	0.09	0.27	9.41

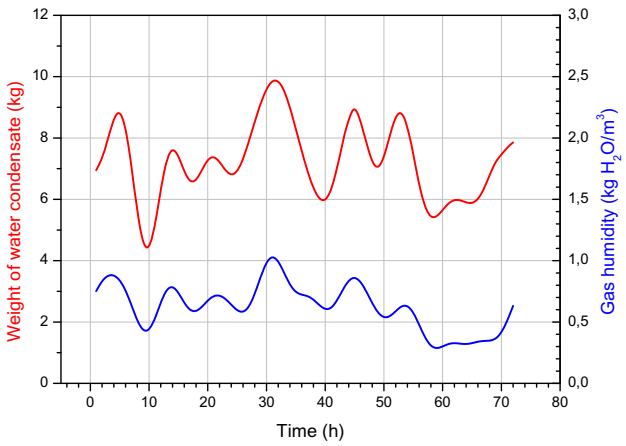

Fig. 7 Weight of water condensate and humidity of process gas

moisture contained in the gasified coal close to the ignition place. As time passed, the gasification zone expanded, the temperature increased, and as a result, the mass of the condensate also increased.

Between 26–32 h, a rapid increase in the weight of the condensate was observed with a maximum of 10 kg/h in 30 h. This stage is most likely related to the increase in temperature of the gasified coal seam and the evaporation of part of the moisture from the wet sand surrounding the coal seam. As the gasification zone expanded, the wet sand heated more and more, resulting in approximately 7 kg/h of condensate being produced between 40–52 h. The moisture content of the sand decreased, the mass of condensate decreased, and the gasification zone moved to further regions of the coal seam. At the end of the process, starting from approximately 58 h, the amount of water released increased again. During the whole process, 521 kg of condensate was obtained, and its average rate of release was approx. 7.2 kg/h. On the basis of the mass of the separated condensate, the moisture content in the process gas was calculated. The shape of this dependence is similar to the curve of the condensate release. The course of the curve has a declining tendency that results from the increasing amount of the process gas. The average calculated moisture content in the process gas converted into dry gas was 0.62 kg H_2O/m^3.

3.4 Determination of CO_2 content in siderite interlayer after gasification process

After the process, samples of thermally transformed siderite were taken again to re-determine the CO_2 content. The samples taken came from the same locations as for the determination of CO_2 content before gasification. This allowed us to compare the CO_2 content in the siderite layer before and after the process. The composition of the separated CO_2 was additionally controlled by a gas chromatograph. The results are presented graphically in Fig. 8 in the form of isolines of CO_2 concentrations in the siderite layer (top view).

The largest decreases in CO_2 content were observed mainly in the first half of the gasified coal seam close to the fire channel located underneath. The farther away from the fire channel, the lower the thermal transformation of siderite. Figure 8 also shows local and lateral deviations of the gasification directions. This direction usually follows the flow direction of the gasifying agent because the oxygen concentration in this stream is the highest. The visible deviations are most likely due to local, higher oxygen concentrations in these areas, which intensified the gasification reaction in these places. The higher the gasification intensity, the higher the temperatures and the higher the level of thermal degradation of the siderite. As a result, the CO_2 content in the siderite layer was located in areas where temperatures were high. This suggests that in real conditions, such a phenomenon may also occur.

The most visible changes in CO_2 concentration occurred from 0–0.5 m and between 1–1.7 m long of the siderite interlayer. In these areas, the CO_2 content fell to the lowest value of 0%–2% by mass. Starting from the length of 1.7 m, the CO_2 content in the siderite layer gradually increased, which means that the farther away from the beginning of the deposit, the smaller the amount of siderite that decomposed to CO_2. This indicates a gradual decrease in the gasification process temperature in these areas. Using data on the CO_2 content in siderite before the process (34.6% by mass) and the data from Fig. 8, it was calculated that only approximately 34.1% of the used siderite was decomposed to CO_2, producing 8.99 m^3 $\pm$ 2 m^3 of CO_2. This represents approximately 2.9%–4.5% of the total amount of CO_2 produced in gasification. This is a small

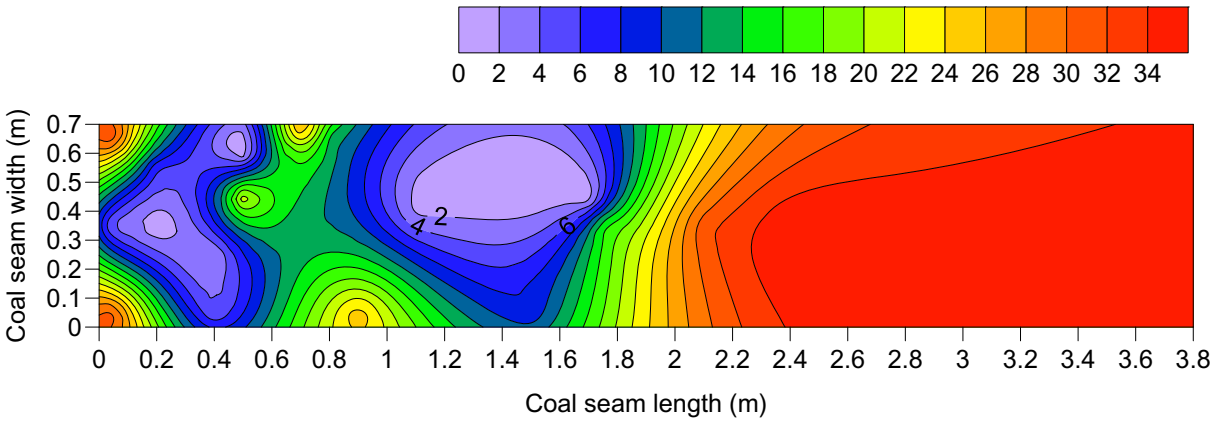

Fig. 8 Isolines of carbon dioxide content in siderite layer after gasification process (wt%)

amount that has little effect on the CO_2 balance and the course of the process.

3.5 Pressure and temperature profiles

The following pictures (Figs. 9, 10, 11, 12) show the pressure and temperature diagrams during the gasification process.

To prevent the air from being sucked in by the suction fan (Fig. 1), the experiment was carried out in such a way that a minimum overpressure of 5–10 hPa was maintained in the reactor. The pressure diagram (Fig. 9a) shows that between hours 10–15 and 48–56 of the process, quite rapid pressure peaks were observed.

Figure 10 shows the temperatures obtained in the lowest layer of the gasified coal seam. The highest temperatures in this layer were recorded by thermocouple T2 at over 1100 °C. The next diagram (Fig. 11) shows the temperature profiles in the second row of thermocouples. These thermocouples were located at a height of approximately 0.3 m from the bottom of the gasified coal seam. The highest temperatures in the second row of thermocouples were recorded by thermocouple T9 and the maximum indicated temperatures were over 1200 °C. Other thermocouples in this row recorded lower values. The third row of thermocouples (T15–21) was located above the layer of siderite in the coal seam at a height of approximately 0.55 m from the bottom. The temperature measurement results recorded by these thermocouples are shown in Fig. 12.

The maximum measured temperatures in the third layer were up to approximately 300 °C. The exception is the second T16 thermocouple, which measured a temperature of approximately 1000 °C. The highest temperature increases were recorded by the thermocouples T2, T9 and T16, which were located at a distance of about 1.2 m from the beginning of the coal block. For the thermocouples

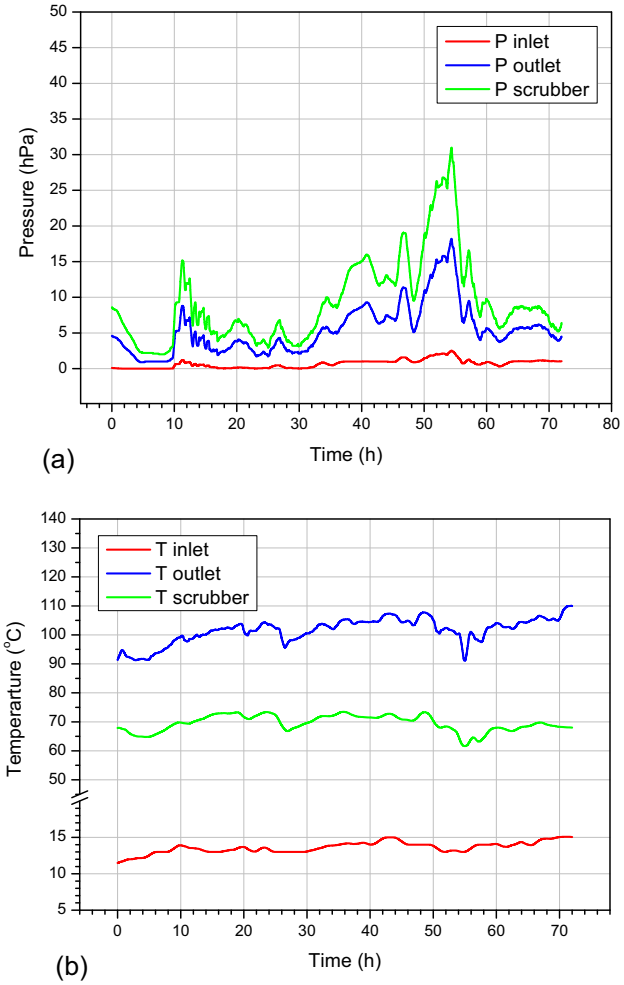

Fig. 9 Pressures and temperatures at reactor inlet, outlet and inside scrubber: **a** pressures, **b** temperatures

located closest to the oxygen inlet to the reactor (T8 and T15), this effect was not observed. It was due to the location of the ignition point which was located near the T2 thermocouple, the direction of oxygen injection and the

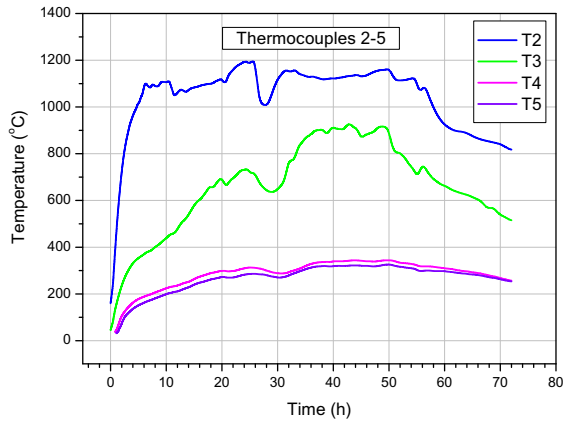

Fig. 10 Temperature graph in fire channel, first row of thermocouples

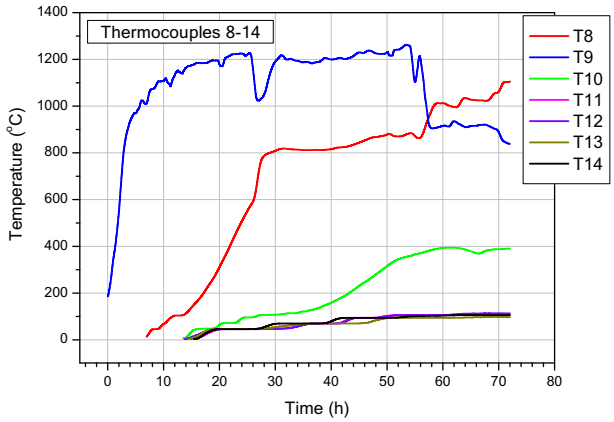

Fig. 11 Temperature diagram in second row of thermocouples

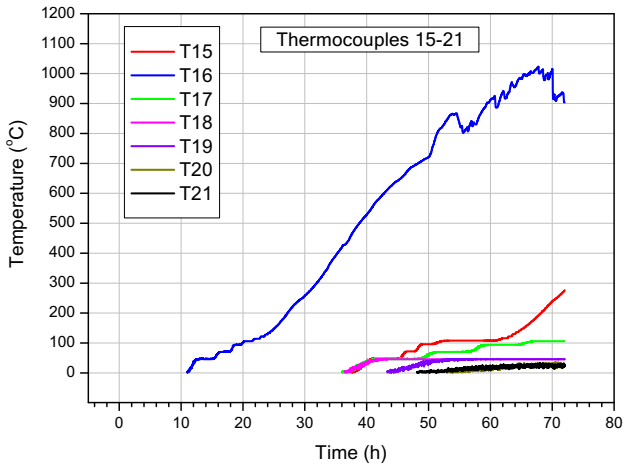

Fig. 12 Temperatures in third layer of thermocouples over siderite interlayer

operating suction fan. Therefore, the direction of gasification and temperature rise was more preferred towards the reactor outlet than towards the oxygen injection. Figures 2a,b 10, 11, 12, 13 show that the T2, T8, T9 and T16

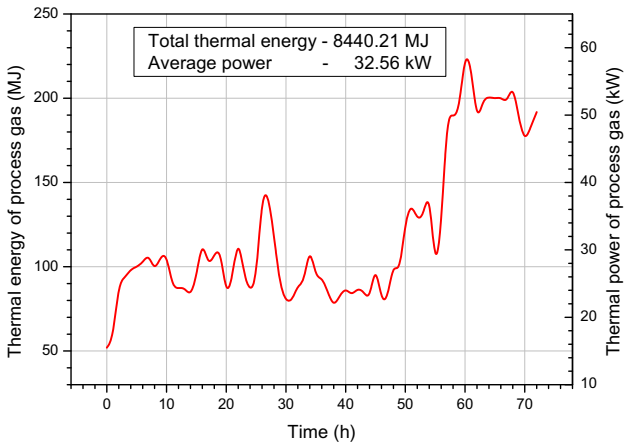

Fig. 13 Heat energy contained in process gas and its heating power

thermocouples were located in the zones where the most carbon dioxide was released from siderite. These thermocouples indicated values exceeding 500 °C. Because siderite decomposes already at this temperature, it is clear that there is a certain correlation between the temperature in these places and the amount of CO_2 released from the siderite.

3.6 Balance calculation

3.6.1 Energy and power

The amount of thermal energy contained in the process gas (after it burned) was calculated on the basis of data on the process gas stream and its calorific value. Then, by dividing the result obtained by the whole gasification time (72 h), the thermal power of the gasification experiment was calculated. The obtained results are shown in Fig. 13. Until approximately 46 h had elapsed, the process gas had a relatively high thermal energy at 100–140 MJ. Starting from the 46th hour of the process, the energy contained in the gas began to increase to a high value of approximately 200 MJ. The calculated average heating power of the process gas obtained during the whole experiment was 32.56 kW.

3.6.2 Coal balance

The process gas contained 327.17 kg of carbon. The coal balance showed that if such a quantity of coal was contained in the process gas, then 532.80 kg of raw coal had to be gasified. Taking into account that the calorific value of coal subjected to gasification was 22.719 MJ/kg, it can be calculated that if such a quantity of coal was burned, then 12,104.82 MJ of thermal energy would be released. It was

calculated that the gasification efficiency was 69.73%. The mass and energy balance results are presented in Table 5.

This is a very good result because it means that only approximately 30% of the energy contained in the calculated amount of gasified coal was used to heat the coal seam to a sufficiently high temperature, evaporate the water and lose to the surrounding strata. On the basis of data on the amount of coal contained in the gasified coal seam before gasification and in the gases obtained, it was calculated that only 23.17% of the total mass of raw coal contained in the reactor was gasified.

3.6.3 Hydrogen balance

The 896.94 m^3 of process gas contained 30.86 kg of hydrogen. 532.80 kg of raw coal containing 4.39% hydrogen was gasified. This amount can theoretically produce 22.98 kg of hydrogen. The missing amount of hydrogen (7.88 kg) could have come from the evaporation of part of the water contained in the coal seam and its reaction with glowing coal. The raw coal used contained 4.70% moisture, and 532.80 kg of coal contained 25.04 kg of water. This amount of water contained 2.78 kg of hydrogen (H_2). The total mass of hydrogen was 25.76 kg. In the balance sheet, 5.10 kg of hydrogen was still missing. However, it is difficult to assume that this calculated amount of water reacted with coal. A large part of it could evaporate and liquefy in the scrubber. It is more likely that the missing amount of hydrogen came from the reaction with coal of part of the water contained in wet sand. Figure 8 shows that the greatest changes in the CO_2 content in the siderite layer occurred in the length of the coal deposit of 1.7 m. These changes are mainly due to the highest temperatures prevailing in this area during gasification. To estimate the amount of water evaporated from the sand, the initial 1.7 m of coal deposit length was taken into account.

In the immediate surroundings of this part of the coal seam, there was approximately 1600 kg of wet sand containing 176 kg of water. This amount of water can theoretically produce19.6 kg of hydrogen. Since only 5.10 kg of hydrogen was missing in the balance, it can be estimated that only approximately 26% of this amount of water reacted to hydrogen, and the rest condensed in the scrubber. It should be taken into account that the calculations made are only approximate, as they do not take into account all factors that may have influenced the results.

3.6.4 Water balance

During the whole experiment, 521 kg of water was condensed in the scrubber. Raw coal in the reactor (2300 kg) contained approximately 108 kg of water. Even if all of this water was evaporated and condensed in the scrubber, 413 kg of water was still missing. The only source of such water is the moisture contained in wet sand. Assuming the simplifying assumption that all of the water contained in 7900 kg of wet sand was evaporated, it was calculated that approximately 869 kg of water could be released from this amount of wet sand. In addition, after taking into account that 46 kg of this water can supplement the hydrogen balance (producing the missing 5.10 kg of hydrogen), 823 kg of water was still available. This amount twice exceeds the water deficiency (413 kg) in the balance. This result proves that the main source of water obtained from gasification is water from wet sand and confirms previous assumptions that part of this water is in the form of steam reacted with coal to water gas, thus increasing the amount of hydrogen and carbon monoxide produced.

3.6.5 Overall mass balance

In order to prepare a mass balance of the process, after the gasification process was completed, the amount of carbon, siderite and sand remaining in the reactor was determined using the weight method. Weighing accuracy was ± 1 kg. The results are shown in Table 6.

The mass balance shows that the total amount of products obtained is 160 kg lower than the total amount of feed to the reactor, which is 1.48%. This difference is very small, which proves the correctness of the measurements and calculations made. The obtained data show that after the process about 279 kg of water remained in the sand, which means that the average humidity of the sand was 3.82%. Because the sand moisture content before the process was 11%, it means that 590 kg of water was lost from the sand during gasification. This amount is admittedly lower than that assumed in Sect. 3.6.4. The total amount of water (869 kg) that can evaporate from wet sand during

Table 5 Mass and energy balance results

Time (h)	Processgas yield (m^3)	Average process gas flow rate (m^3/h)	Average process gas calorific value (MJ/m^3)	Total heat energy in the process gas (MJ)	Average reactor operating power (kW)	Average gasification rate (kg/h)	Energy contained in coal gasified (MJ)	Gasification energy efficiency (%)
72	896.94	12.46	9.41	8440.21	32.56	7.40	12,104.82	69.73

Table 6 Overall mass balance

Parameter	Value (kg)
Input	
Raw coal	2300
Siderite	150
Wet sand of 11% humidity	7900
Oxygen injected	463
Total input	10,813
Output	
Coal after gasification	1735
Siderite after gasification	129
Sand	7310
Process gas	958
Liquid condensate	521
Total output	10,653
Difference between input and output	160

gasification, but still exceeds the missing 413 kg in the water balance. This result confirms that the main source of water in this coal gasification process was water contained in wet sand.

The accuracy of the mass balance could be influenced by many factors, the most important of which are errors in the measurement of the following data:

(1) mass of coal, siderite and sand,
(2) technical and elemental composition of coal,
(3) moisture content in sand,
(4) composition and amount of gas produced,
(5) oxygen flow rate,
(6) volume of water flowing to the scrubber and waste water generated during gasification.

4 Discussion of results obtained

On the basis of the results obtained, the influence of the siderite interlayer on the amount and composition of the process gas was not found. This is because an insufficient amount of CO_2 separated from the siderite layer. The puzzling sudden decreases in the concentration of carbon dioxide in the process gas are shown in Fig. 5. There may be several reasons for this. For example, increasing the temperature of the gasified coal seam above 650 °C produces a Bouduard reaction that leads to an increase in carbon monoxide content. However, Fig. 5 shows that with an increase in CO concentration, the H_2 concentration increases at the same time. Thus, it is more probable that under the described conditions, with a large supply of steam, the production of water gas ($H_2 + CO$) was preferred over CO production alone. This was also confirmed during the water balance calculation in this process. The required temperature for water gas formation is 700–900 °C. Such temperatures were recorded during this gasification process, and therefore the production of combustible components of this gas was possible. The results obtained indicate the important role of water in the underground gasification process. In the case of this experiment, its source was the moisture contained in the sand surrounding the gasified coal seam; however, under real conditions, in the absence of this moisture, it must be supplied from outside. The results obtained were also influenced by the correct operation of the reactor's oxygen supply system and the removal of produced gases from the reactor. Properly selected conditions of cooperation of both these systems also contributed to the high energy efficiency of the whole gasification process.

5 Conclusions

(1) Due to the small amount of CO_2 produced from the thermal decomposition of the siderite interlayer, its influence on the coal gasification process was not observed. However, based on the differences in the CO_2 content in the siderite interlayer before and after the process, it was found that the gasification direction may differ from the gasification agent flow direction. This phenomenon may occur in the case of a real underground gasification process.
(2) The use of wet sand to surround the gasified coal had an important impact on the gasification process. The water contained in the wet sand reacted with the coal, producing large amounts of hydrogen and carbon monoxide, which improved the amount and composition of the gas as well as the energy balance of the process. This result shows the important role of water, which is necessary in the UCG process.
(3) One of the important factors influencing the course of the process was the suitably fast take of the process gas produced. Efficient operation of this installation also contributed to the high efficiency of the gasification process.

Author's contribution MW: Conceptualization, validation, investigation, writing—original draft. KK: methodology, visualization, supervision, project administration. JN: conceptualization, validation, investigation, formal analysis. MS: methodology, resources, investigation, funding acquisition. WB: formal analysis, investigation, data curation, writing—review and editing. All authors have read and agreed to the published version of the manuscript.

Funding The research presented in this article was performed within the work "Conducting an exsitu experiment of underground coal gasification with a mineral interlayer" commissioned and funded by the Silesian University of Technology in Gliwice, Department of Applied Geology, by order sign ZP/018521/18/ZZ/01987/18.

Declarations

Conflict of interest The authors declare that they have no known competing financial interests or personal relationships that could have appeared to influence the work reported in this paper.

Ethical approval The experiments comply with the current laws of Poland.

References

Bhutto AW, Bazmi AA, Zahedi G (2013) Underground coal gasification: from fundamentals to applications. Prog Energy Combust Sci 39:189–214

Blinderman MS, Friedmann SJ (2006) Underground coal gasification and carbon capture and storage: technologies and synergies for low-cost, low-carbon syngas and secure storage. Lawrence Livermore National Laboratory [Report UCRL-ABS-218560]

Cena RJ, Thorness CB (1981) Underground coal gasification Data Base. Lawrence Livermore National Laboratory, Livermore CA 94550

Chodyniecka L, Gabzdyl W (1986) Komunikat o syderytach z kopalni "Czeczot". Zeszyty Naukowe Pol. Śląskiej nr 900, Górnictwo z. 149, Gliwice, 511–518 (**in Polish**)

Chodyniecka L, Walanus A (1985) Mineralogical characteristics and origin of sideritic concretions from the "Szczygłowice" coal mine. Upper Silesia Mineralogia Polonica 16(1):77–83

Daggupati S, Mandapati RN, Mahajani SM, Ganesh A, Sapru RK, Sharma RK, Aghalayam P (2011) Laboratory studies on cavity growth and product gas composition in the context of underground coal gasification. Energy 36:1776–1784

Dhupe AP, Gokarn AN (1990) Studies in the thermal decomposition of natural siderites in the presence of air. Int J Miner Process 28:209–220

Dvornikova EV (2018) The role of groundwater as an important component in underground coal gasification. Underground Coal Gasification and Combustion 253–281

Elliott MA (1981) Chemistry of coal utilization. 2nd Suppt. United States

Gregg DW, Edgar TF (1978) Underground coal gasification. AIChE J 24:753–781

Hamanaka A, Su F, Itakura K, Takahashi K, Kodama J, Degouchi G (2017) Effect of injection flow rate on product gas quality in underground coal gasification (UCG) based on laboratory scale experiment: development of co-axial UCG system. Energies 10(2):238

Hildebrandt R (2015) Sposób rozruchu georeaktora podziemnego zgazowania węgla. Wiadomości Górnicze 11:593–596 ((**in Polish**))

Huang W, Wang Z, Duan T, Xin L (2021) Effect of oxygen and steam on gasification and power generation in industrial tests of underground coal gasification. Fuel 289:1–12

Kapusta K, Wiatowski M, Stańczyk K (2016) An experimental ex-situ study of the suitability of a high moisture ortho-lignite for underground coal gasification (UCG) process. Fuel 179:150–155

Kapusta K, Wiatowski M, Zagoršćak R, Thomas HR (2020) Large-scale experimental investigations to evaluate the feasibility of producing methane-rich gas (SNG) through underground coal gasification process. Effect of coal rank and gasification pressure. Energies 13:1334

Karimi A, Gray MR (2011) Effectiveness and mobility of catalysts for gasification of bitumen coke. Fuel 90:120–125

Kreinin EV, Fedorov NA, Zvyagintsev KN, Pyankova TM (1982) Underground gasification of coal seams. Nedra, Moscow (in Russian)

Lee JY, Lee DW, Lee KY, Wang Y (2009) Cr-free Fe-based metal oxide catalysts for high temperature water gas shift reaction of fuel processor using LPG. Catal Today 146(1–2):260–264

Maes II, Gryglewicz G, Yperman J, Franco DV, Haes JH, D'Oliveslaeger M, van Poucke LC (2000) Effect of siderite in coal on reductive pyrolytic analyses. Fuel 79:1873–1881

Maev S, Bliderman MS, Gruber GP (2018) Underground coal gasification (UCG) to products: designs, efficiencies, and economics. Underground Coal Gasification and Combustion 435–468

Mandapati RN, Daggupati S, Mahajani SM, Aghalayam P, Sapru RK, Sharma RK, Ganesh A (2012) Experiments and kinetic modeling for CO_2 gasification of indian coal chars in the context of underground coal gasification. Ind Eng Chem Res 51(46):15041–15052

Mocek P, Pieszczek M, Świądrowski J, Kapusta K, Wiatowski M, Stańczyk K (2016) Pilot-scale underground coal gasification (UCG) experiment in an operating Mine „Wieczorek" in Poland. Energy 111:313–231

Olness D (1982) The Angrenskaya Underground Coal Gasification Station. Lawrence Livermore Laboratory, University of California. Livermore, California 94550

Perkins G (2018) Underground coal gasification—part I: field demonstrations and process performance. Prog Energy Combust Sci 67:158–187

Perkins G, Prabu V (2017) Considerations for oxidant and gasifying medium selection in underground coal gasification. Fuel Process Technol 165:145–154

Retallack GJ (2007) Coevolution of life and earth". In: Stevenson D (ed) Treatise of geophysics: earth evolution. Elsevier, Amsterdam, pp 295–320

Riley KW, French DH, Farrell OP, Wood RA, Huggins FE (2012) Modes of occurrence of trace and minor elements in some Australian coals. Int J Coal Geol 94:214–224

Roberts DG, Harris DJ (2000) Coal gasification with O2, CO2, and H2O: effects of pressure on intrinsic reaction kinetics. Energy Fuels 14(2):483–489

Shu X, Li J, Hao J, Liu Z, Wang Q, Lu X (2020) Effect of atmosphere and temperature on syngas production during gasification of Zhundong lignite and water-washed Zhundong lignite in a fixed-bed reactor. Chem Pap 74:555–569

Smirnov AN, Klochkovsky SP, Krylova SA, Sysoev VI (2019) Gasification of the Kuznetsk basin coal concentrate using oxide iron–magnesium catalysts. J Chem Technol Metall 54(2):286–291

Su F, Hamanaka A, Itakura K, Degouchi G, Sato K (2017) Evaluation of coal combustion zone and gas energy recovery for underground coal gasification (UCG) process. Energy Fuels 31(1):154–169

Surya Kanta D, Prabu V (2017) Experimental studies on humidified/water influx O2 gasification for enhanced hydrogen production in the context of underground coal gasification. Int J Hydrogen Energy 42:14089–14102

Wall TF, Liu G-S, Wu H-W, Roberts DG, Benfell KE, Gupta S et al (2002) The effects of pressure on coal reactions during pulverized coal combustion and gasification. Prog Energy Combust Sci 28(5):405–433

Wang ZT, Ding XP, Huo LW, Wang GX, Rudolph V (2008) A remining technology of underground coal gasification At Zhongliangshan Coal Mine. J Coal Sci Eng 14(3):469–473

Wang YL, Zhu SH, Gao MQ, Yang ZR, Yan LJ, Bai YH, Li F (2016) A study of char gasification in H_2O and CO_2 mixtures: Role of inherent minerals in the coal. Fuel Process Technol 141:9–15

Wang Z, Liang J, Shi L, Xi J, Li S, Cui Y (2017) Expansion of three reaction zones during underground coal gasification with free and percolation channels. Fuel 190:435–443

Wiatowski M, Kapusta K, Świądrowski J, Cybulski K, Ludwik-Pardała M, Grabowski J, Stańczyk K (2015) Technological aspects of underground coal gasification in the Experimental "Barbara" Mine. Fuel 159:454–462

Wiatowski M, Kapusta K, Ludwik-Pardała M, Stańczyk K (2016) Ex-situ experimental simulation of hard coal underground gasification at elevated pressure. Fuel 184:401–408

Yang LH, Zhang X, Liu S (2009) Underground coal gasification using oxygen and steam. Energy Sour Part A Recov Util Environ Eff 31(20):1883–1892

Zhu D, Luo Y, Pan J, Zhou X (2016) Reaction mechanism of siderite lump in coal-based direct reduction. High Temp Mater Proc 35(2):185–194